Potentiation of GABAergic synaptic transmission by AMPA receptors in mouse cerebellar stellate cells: changes during development

Ingrid Bureau and Christophe Mulle

CNRS UMR 5541, Université Victor Segalen-Bordeaux 2, 146 rue Léo-Saignat, 33076 Bordeaux, France

(Received 30 April 1997; accepted after revision 3 March 1998)

1. The effects of low concentrations of domoate, an agonist at both α-amino-3-hydroxy-5-methylisoxazole-4-propionate and kainate receptors (AMPARs and KARs, respectively), were investigated in stellate cells in slices of mouse cerebellum at two developmental stages (postnatal day (PN) 11–13 and PN21–25).

2. Low concentrations of domoate enhanced the frequency of miniature IPSCs (mIPSCs) recorded in the presence of tetrodotoxin (TTX) at PN11–13 but not at PN21–25.

3. The effects of low concentrations of domoate on synaptic activity were probably mediated by the activation of AMPARs and not KARs, since they were blocked by GYKI 53655 (LY300168), a selective AMPAR antagonist.

4. Domoate increased mIPSC frequency in part by activation of presynaptic voltage-dependent Ca^{2+} channels since potentiation was reduced by 60% in the presence of Cd^{2+}. AMPARs in stellate cells were found to be permeable to Ca^{2+}. The residual potentiation in the presence of Cd^{2+} could thus be due to a direct entry of Ca^{2+} through AMPAR channels.

5. In the presence of TTX, potentiation of synaptic activity by focal application of domoate was not restricted to the region of the cell body, but was observed within distances of 120 μm. These experiments also revealed a strong spatial correlation between the location of the presynaptic effects of domoate and the activation of postsynaptic AMPARs.

6. Our data show a developmentally regulated presynaptic potentiation of synaptic transmission between cerebellar interneurones mediated by AMPARs. We discuss the possibility that the developmental switch could be due to a shift in the localization of AMPARs from the axonal to the somato-dendritic compartment.

In mammals, stellate and basket cells are two types of small interneurones present in the molecular layer of the cerebellum. Both types of interneurones are GABAergic and constitute the major inhibitory input to Purkinje cells (Palay & Chan-Palay, 1974). They receive an excitatory input from the parallel fibres and their major inhibitory input from other basket and stellate cells. Basket cells are located close to the Pukinje cell layer, while stellate cells are found in the outer two-thirds of the molecular layer. Although basket cells might receive a GABAergic input from Purkinje cell axon collaterals in addition to the GABAergic input from other stellate and basket cells, the synaptic physiology of basket and stellate cells has numerous features in common (Llano & Gerschenfeld, 1993*a*).

General distribution studies of genes encoding α-amino-3-hydroxy-5-methylisoxazole-4-propionate (AMPA) and kainate (KA) receptor (respectively, AMPAR and KAR) subunits by *in situ* hybridization have shown high expression of the GluR3 AMPAR subunit (Keinänen *et al.* 1990; Sato, Kiyama & Tohyama, 1993), and a moderate level of GluR2 subunit expression in stellate and basket cells. Consistent with these observations, labelling with GluR1- and GluR4-subunit-specific antibodies has confirmed the absence of these subunits in stellate and basket cells, which were most densely stained with a GluR2/3 antibody (Petralia & Wenthold, 1992; Baude, Molnar, Latawiec, McIlhinney & Somogyi, 1994), while labelling with a GluR2-specific antibody has revealed a virtual absence of the GluR2 subunit in these cells (Petralia, Wang, Mayat & Wenthold, 1997). In addition, stellate and basket cells are one of the few populations of neurones in the brain that show a high level of expression of the GluR7 subunit gene of the KAR family (Bettler *et al.* 1992; Wisden & Seeburg, 1993), with no significant expression of the other KAR subunit genes.

In this paper, we have initiated a study on the functional characteristics of AMPARs and KARs in stellate cells.

AMPARs mediate excitatory synaptic transmission at the great majority of excitatory synapses in the vertebrate central nervous system. Immunolabelling with receptor antibodies has confirmed that AMPARs are restricted to dendritic postsynaptic densities, at least in the adult (Petralia & Wenthold, 1992). The role of KARs in synaptic transmission is unclear. Two recent studies have disclosed a synaptic activation of KARs, presumably located at a postsynaptic site, in CA3 hippocampal neurones (Castillo, Malenka & Nicoll, 1997; Vignes & Collingridge, 1997). However, a number of studies suggest that KARs influence synaptic transmission by acting at a presynaptic site (Represa, Tremblay & Ben-Ari, 1987; Gaiarsa, Zagrean & Ben-Ari, 1994; Chittajallu, Vignes, Dev, Barnes, Collingridge & Henley, 1996) as opposed to AMPARs whose action is considered to be strictly postsynaptic.

In this study, we have found that domoate increases the frequency of IPSCs in stellate cells in the absence of action potential firing in the presynaptic neurones. We show that this presynaptic modulation of GABAergic synaptic transmission is mediated by AMPARs and not KARs. Interestingly, this effect of domoate is only present in stellate cells from immature mice (postnatal day (PN) 11–13) and disappears in older mice (PN21–25).

METHODS

Parasagittal cerebellar slices (250–300 μm thick) were prepared according to previously described methods (Edwards, Konnerth, Sakmann & Takahashi, 1989; Llano & Gerschenfeld, 1993*a*) from 11- to 25-day-old mice of the Swiss strain. Mice were killed by decapitation after cervical dislocation, and slices were cut from the cerebellar vermis in the sagittal plane in ice-cold oxygenated HCO_3–H_2PO_4-buffered saline (for composition see below). Slices were kept at room temperature (20–25 °C) in oxygenated HCO_3–H_2PO_4-buffered saline for up to 6 h before being transferred to the experimental set-up.

The cerebellar slices were visualized throughout the recording session with an upright micropscope equipped with Nomarski optics (Axioscope, Carl Zeiss, Germany). Tight-seal whole-cell recordings were obtained from neurones visually identified as stellate cells according to their small size and their location in the outer half of the molecular layer. In addition, these cells displayed spontaneous action potentials before breaking into the cells as well as tetrodotoxin (TTX)-sensitive voltage-gated currents in the whole-cell mode. Spontaneous synaptic currents were observed under control conditions. Focal stimulation using a patch electrode placed in the vicinity of the recorded neurone yielded GABAergic and 6-cyano-7-nitroquinoxaline-2,3-dione-sensitive synaptic currents (data not shown). These morphological and physiological criteria identified these neurones as being stellate cells (Llano & Gerschenfeld, 1993*a*). Recordings were performed at room temperature. The slice was continuously perfused with a physiological saline of the following composition (mM): 125 NaCl, 2·5 KCl, 2 $CaCl_2$, 1 $MgCl_2$, 1·25 NaH_2PO_4, 26 $NaHCO_3$, 25 glucose and 0·2 ascorbic acid (pH 7·4 when bubbled with a mixture of 95% O_2 and 5% CO_2). For Ca^{2+} permeability measurements, Hepes-buffered solutions were used. The Na^+-rich solution contained (mM): 135 NaCl, 5·6 KCl, 2 $CaCl_2$, 1 $MgCl_2$ and 5 Hepes; pH adjusted to 7·3 with NaOH. The 100 mM $CaCl_2$-rich solution contained (mM): 100 $CaCl_2$ and 5 Hepes; pH adjusted to 7·3 with $Ca(OH)_2$. Whole-cell voltage-clamp and nucleated patch (Sather, Dieudonné, MacDonald & Ascher, 1992) recordings were performed with a caesium-based internal solution containing (mM): 140 CsCl, 2 $MgCl_2$, 1 $CaCl_2$, 10 EGTA, 10 Hepes and 2 Na-ATP (pH 7·3). Recording patch electrodes were pulled from borosilicate glass and had resistances of 2·3–3·2 MΩ when filled with the CsCl-based solution. For current-clamp recordings, KCl was substituted for CsCl in the internal solution.

Whole-cell membrane currents were recorded with an EPC9 amplifier (HEKA, Germany) driven by a MacIntosh PowerPC computer. Stellate cells were voltage clamped at a holding potential of −70 mV, unless otherwise stated. Capacitance transients were automatically cancelled by the EPC9 program. Series resistance was $12{\cdot}7 \pm 0{\cdot}8$ MΩ ($n = 39$) and was not compensated, but was controlled throughout the recording session. Since the amplitude of most synaptic currents was lower than 500 pA the DC resistance error was not greater than 6 mV. Extracellular recordings of action potentials were performed in the cell-attached configuration.

Spontaneous synaptic currents, extracellular action potentials and voltage data were filtered at 10 kHz, digitized at 100 or 250 μs point^{-1} and acquired continuously on a computer hard disk using 'Pulse' program (HEKA). The detection and analysis of spontaneous synaptic currents were performed using Detectivent, a program written by N. Ankri (Ankri, Legendre, Faber & Korn, 1994). Data were further analysed using macros written for IGOR (Wavemetrix Inc., USA). The permeability ratio (P_{Ca}/P_{Na}) was determined from the reversal potentials in the Na^+-rich extracellular solution ($V_{rev,Na}$) and the Ca^{2+}-rich extracellular solution ($V_{rev,Ca}$) using the following equation:

$$P_{Ca}/P_{Na} = 1/4\{a^{o}_{Na}/a^{o}_{Ca}[\exp((2V_{rev,Ca} - V_{rev,Na})F/RT) + \exp((V_{rev,Ca} - V_{rev,Na})F/RT)]\},$$

where a^{o}_{Na} (extracellular sodium activity) is 0·75 for 135 mM Na^+ and a^{o}_{Ca} (extracellular calcium activity) is 0·515 for 100 mM Ca^{2+} (Geiger *et al.* 1995; and references therein). The universal gas constant (R), absolute temperature (T) and Faraday's constant (F) have their conventional values. The junction potential between the Hepes Na^+-rich solution and the CsCl internal solution, determined using a recording pipette filled with 3 M CsCl solution, was +4·8 mV. The junction potential between the 100 mM Ca^{2+}-rich solution and the Hepes Na^+-rich solution was +5·2 mV. Reversal potentials measured in the 100 mM Ca^{2+}-rich solution were then corrected by −10 mV.

Data are presented as means ± standard error of the mean. Statistical differences between two sets of data were assessed with a Mann–Whitney test and, for paired values, with a Wilcoxon test. $P < 0{\cdot}01$ was considered significant.

For most experiments, pharmacological agents were delivered either by bath perfusion or by means of a multibarrelled gravity-fed system, composed of four to six capillaries, which was positioned just above the slice and could be moved laterally. Exchange of solutions by bath perfusion was achieved within 1–2 min. Using the array of capillaries, application was much faster: a control application of GABA (50 μM) or domoate (50 μM) gave a peak response within 1–2 s in whole-cell experiments (the exchange rate was principally limited by diffusion within the slice). Rapid application of domoate to nucleated patches excised from stellate cell somata was performed using the same multibarrelled system. For focal application of domoate, a patch pipette filled with a solution containing 1 μM domoate and 500 nM TTX was coupled to a Picospritzer II (General Valve Corp., NJ, USA) system. It was

moved above the slice surface, at various distances from the recorded stellate cell body. The distance was measured using a grid in the microscope ocular. In all experiments in which TTX (400–500 nM) was used, TTX was added to the bath perfusion medium as well as to capillaries containing control solutions, in order to ensure that the slice was entirely bathed with TTX. The effect of domoate observed in the presence of TTX could not be attributed to poor block by TTX or incomplete perfusion of the slice. First, the absence of any voltage-gated Na^+ current was regularly monitored in the recorded neurone. These currents can be totally blocked by addition of 100 nM TTX (Llano & Gerschenfeld, 1993), a concentration 4–5 times lower than the concentration used in this study. The blockade of Na^+ currents as well as the sharp decrease in GABAergic PSC frequency was observed within seconds after the beginning of the TTX perfusion, when applied by the fast perfusion system, and was not subject to any slow change after up to 20–40 min of recording.

Most salts and chemicals were obtained from Sigma. Domoate was purchased from Tocris Cookson (Bristol, UK). GYKI 53655 (LY300168) was a generous gift from Lilly Research Laboratories (Indianapolis, IN, USA).

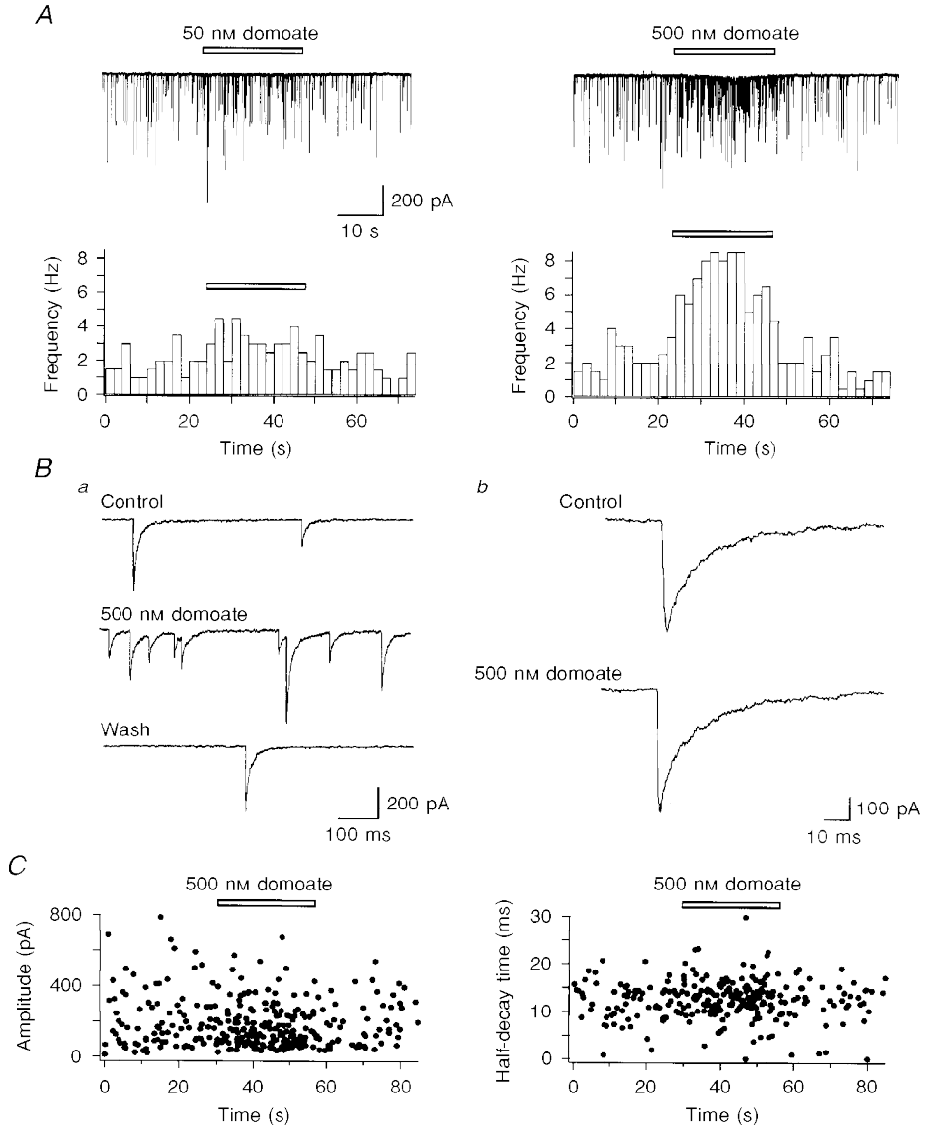

Figure 1. Low concentrations of domoate enhance synaptic activity in cerebellar stellate cells

A, upper panels: samples of a continuous recording of spontaneous PSCs in a stellate cell. Lower panels: plots for the same cell of the mean frequency of PSCs detected during 2 s sample intervals against time. Domoate (50 and 500 nM), applied during the time indicated by the horizontal bars, led to a reversible increase in synaptic activity in a dose-dependent manner. *Ba* and *Bb*, traces displaying, on an expanded time scale, selected portions of the data sample in the right-hand recording in *A*. Only PSCs with a long time course of decay, presumably GABAergic IPSCs, were observed. *C*, amplitude and half-decay time of synaptic events detected in continuous recordings in another cell. Domoate changed the frequency of the synaptic currents without obvious change in the amplitude or the time course of decay. Horizontal bars indicate the time during which 500 nM domoate was applied. Membrane holding potential was −70 mV. All experiments were performed using cells from PN17 mice.

RESULTS

Low concentrations of domoate increase the frequency of spontaneous GABAergic synaptic currents in stellate cells

Whole-cell recordings of stellate cells of the cerebellar molecular layer were performed under direct visual inspection (see Methods). As in the rat (Llano & Gerschenfeld, 1993), most spontaneous synaptic currents were blocked by application of bicuculline (20 μM), which caused a decrease in PSC frequency of $97{\cdot}3 \pm 0{\cdot}7$ % ($n = 4$), and were therefore mediated by the activation of $GABA_A$ receptors (see Fig. 2*A*).

Since stellate/basket cells make synaptic contacts with each other and since they express both AMPAR and KAR subunits, by recording from a single stellate cell we could investigate the effects of the application of domoate on synaptic transmission between stellate cells at a presynaptic level as well as on the activation of postsynaptic AMPARs and/or KARs in these same neurones. Application of domoate at low concentrations (50–500 nM) caused, within a few seconds, a sharp increase in the frequency of synaptic currents in stellate cells (Fig. 1). This barrage of PSCs was observed on top of a very small postsynaptic current (range, 0–11 pA) mediated by direct activation of AMPARs or KARs. Figure 1 shows an example of such recording. The increase in PSC frequency was rapidly reversed upon removal of the agonist and was often followed by a period of reduced synaptic activity. On average, domoate (500 nM) increased the frequency of PSCs by a factor of $3{\cdot}1 \pm 0{\cdot}5$ ($n = 17$). This effect was accompanied by a small decrease in the amplitude of PSCs. The mean ratio of the mean PSC amplitude obtained in domoate over that obtained under control conditions was $0{\cdot}92 \pm 0{\cdot}03$ (range, 0·79 to 1·06; $n = 17$). When the domoate concentration was increased to 1 μM, a more pronounced decrease in the mean PSC amplitude could be observed (see Fig. 3*A*). This aspect was variable from cell to cell and might be attributable to a phenomenon of synaptic fatigue. It was not further analysed.

In the vast majority of cells tested, only an increase in PSCs with slow kinetics of decay (Fig. 1*B* and *C*), presumed to be GABAergic IPSCs, was observed. Application of domoate (250 nM) in the presence of bicuculline failed to induce an increase in synaptic activity, demonstrating that only GABAergic synaptic transmission is potentiated by domoate (Fig. 2*A*).

The GABAergic afferent neurones to stellate cells are known to be neighbouring stellate/basket cells (Palay & Chan-Palay, 1974). In all stellate cells tested, domoate at submicromolar concentrations increased action potential frequency recorded in the cell-attached patch-clamp configuration (data not shown). Stellate cells are known to be compact cells (input resistance, 863 ± 141 MΩ; $n = 7$), allowing very small inward currents (a few picoamps) to depolarize the neuronal membrane to action potential threshold.

The AMPAR antagonist GYKI 53655 (LY300168), which does not affect KAR responses (Paternain, Morales & Lerma, 1995; Castillo *et al.* 1997; Vignes & Collingridge, 1997), completely blocked the domoate-induced increase in

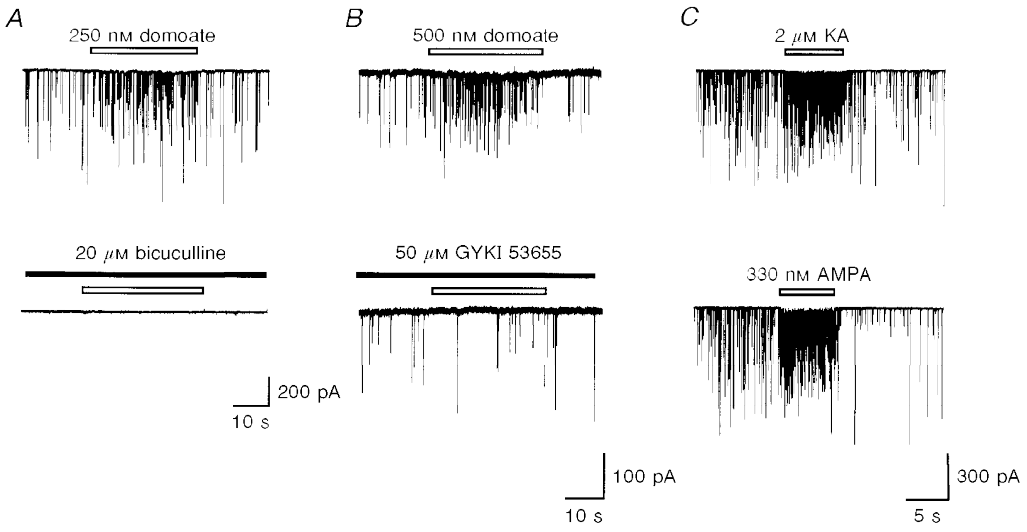

Figure 2. Pharmacology of the effects of domoate on synaptic activity

A, samples of a continuous recording of spontaneous PSCs in a stellate cell. Bicuculline (20 μM) dramatically decreased spontaneous synaptic activity. In the presence of bicuculline (indicated by the filled horizontal bar), no potentiation of synaptic activity was induced by the application of 250 nM domoate (indicated by the open horizontal bars). *B*, addition of GYKI 53655 (50 μM; indicated by the filled horizontal bar) blocked the increase in spontaneous PSC frequency induced by 500 nM domoate. *C*, addition of KA (2 μM) and AMPA (330 nM) (indicated by the horizontal bars) induced a reversible potentiation of synaptic activity. Recordings in *A*–*C* are from 3 differents cells from PN14, PN14 and PN13 mice, respectively.

synaptic activity (Fig. 2*B*), as well as postsynaptic currents activated by micromolar concentrations of domoate (data not shown). In addition, application of KA (2 μM) and AMPA (330 nM) increased the spontaneous IPSC frequency by a factor of $4{\cdot}0 \pm 0{\cdot}9$ ($n = 5$) and $11{\cdot}1 \pm 4{\cdot}2$ ($n = 4$), respectively (Fig. 2*C*). Thus, low concentrations of domoate and KA increase excitability of cerebellar stellate cells by activation of AMPARs but not KARs. In contrast, in hippocampal CA3 neurones, these concentrations of KA mainly activate KARs (Castillo *et al.* 1997).

In immature stellate cells, domoate potentiates synaptic activity in the presence of TTX

We tested whether TTX completely blocked the effect of domoate on IPSC frequency. As described for rat cerebellar interneurones (Llano & Gerschenfeld, 1993*a*), TTX (400–500 nM) completely abolished the TTX-sensitive voltage-activated Na^+ inward currents. Addition of TTX rapidly decreased the frequency of occurrence of IPSCs, as well as the mean amplitude of IPSCs (Fig. 3*B*). Overall, the ratio of the mean amplitude of IPSCs in TTX *versus* control saline was $0{\cdot}69 \pm 0{\cdot}06$ (range, 0·32 to 1·10; $n = 15$). This decrease can be accounted for mainly by the disappearance of IPSCs of larger amplitude and not by a shift in the amplitude of all synaptic events, as already described in the rat by Llano & Gerschenfeld (1993*a*).

In preliminary experiments, we found that domoate (500 nM to 1 μM) increased IPSC frequency in the presence of TTX (Fig. 3*C*) in immature stellate cells (PN11–15). The effect of domoate in the presence of TTX could not be attributed to poor block by TTX or incomplete perfusion of

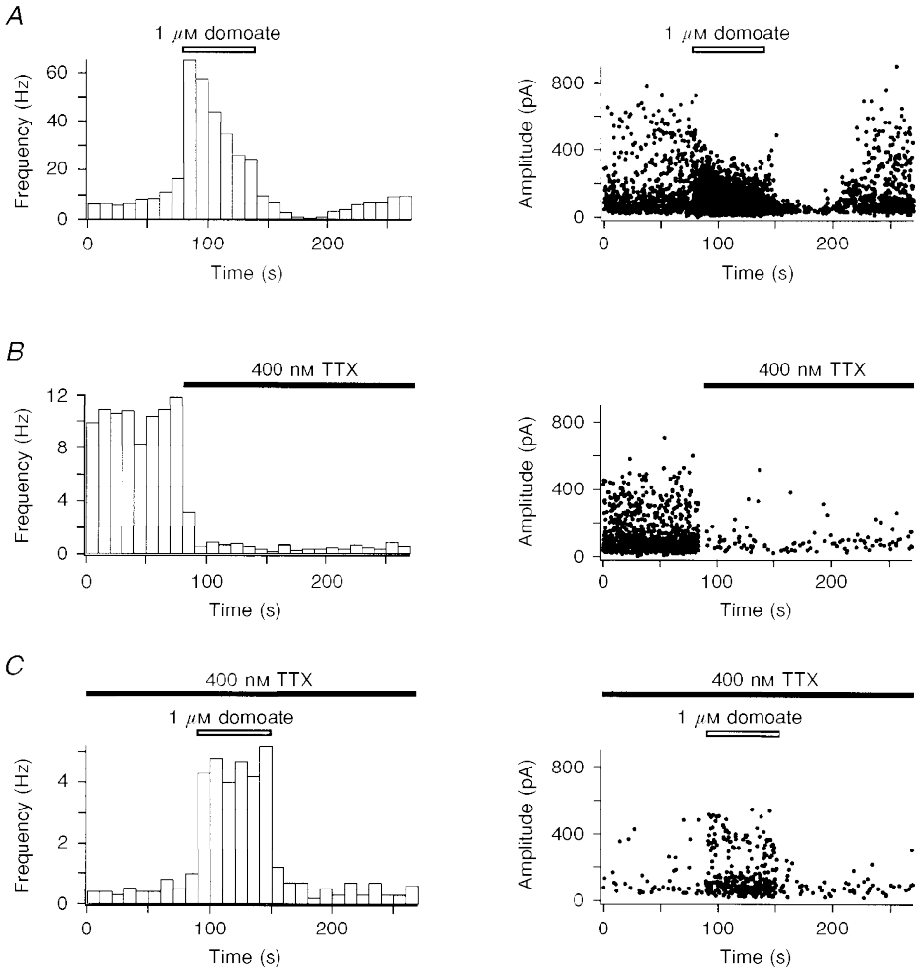

Figure 3. Domoate increases the frequency of miniature IPSCs (mIPSCs) in stellate cells

Left panels: plots of the mean frequency of synaptic events detected during 10 s intervals against time. Right panels: plots of the amplitude of single IPSCs recorded continuously. All data are from the same neurone from a PN12 mouse. *A*, addition of domoate (1 μM) induced a large increase in spontaneous IPSC frequency which was followed, in this neurone, by a reversible decrease in synaptic activity as well as in IPSC amplitude that outlasted the application of domoate. *B*, in the same cell, addition of 400 nM TTX dramatically decreased spontaneous synaptic activity. *C*, in the presence of TTX, domoate induced an increase in the frequency of mIPSCs. The slice was bathed in physiological saline supplemented with 400 nM TTX.

the slice (see Methods). We thus investigated in greater detail the effects of low concentrations of domoate on synaptic activity during the course of maturation, between PN11, a day or two after final neurogenesis of stellate cells (Altman & Bayer, 1997), and PN25.

The basal level of IPSC frequency increased with the age of the animal from $1{\cdot}6 \pm 0{\cdot}7$ Hz at PN11–13 ($n = 6$) to $10{\cdot}3 \pm 2{\cdot}9$ Hz at PN21–25 ($n = 7$) (Figs 4 and 5). During the same period, the frequency of mIPSCs (recorded in the presence of 500 nM TTX) increased from $0{\cdot}21 \pm 0{\cdot}03$ Hz at PN11–13 ($n = 13$) to $1{\cdot}30 \pm 0{\cdot}43$ Hz at PN21–25 ($n = 7$). Interestingly, the ratio of the frequency of mIPSCs over that of spontaneous IPSCs did not change with age (0·13 at PN11–13 and at PN21–25). If the developmental increase in the frequency of spontaneous IPSCs was due to an increase in the overall level of spike discharge in the individual presynaptic interneurones, one would not expect to observe a parallel increase in the frequency of mIPSCs. In addition, we found no notable change in the level of spike discharge activity in individual stellate cells between PN13 and PN25 (data not shown). A more likely explanation for the parallel increase in the frequency of IPSCs and mIPSCs is that, during the course of this phase of development, the

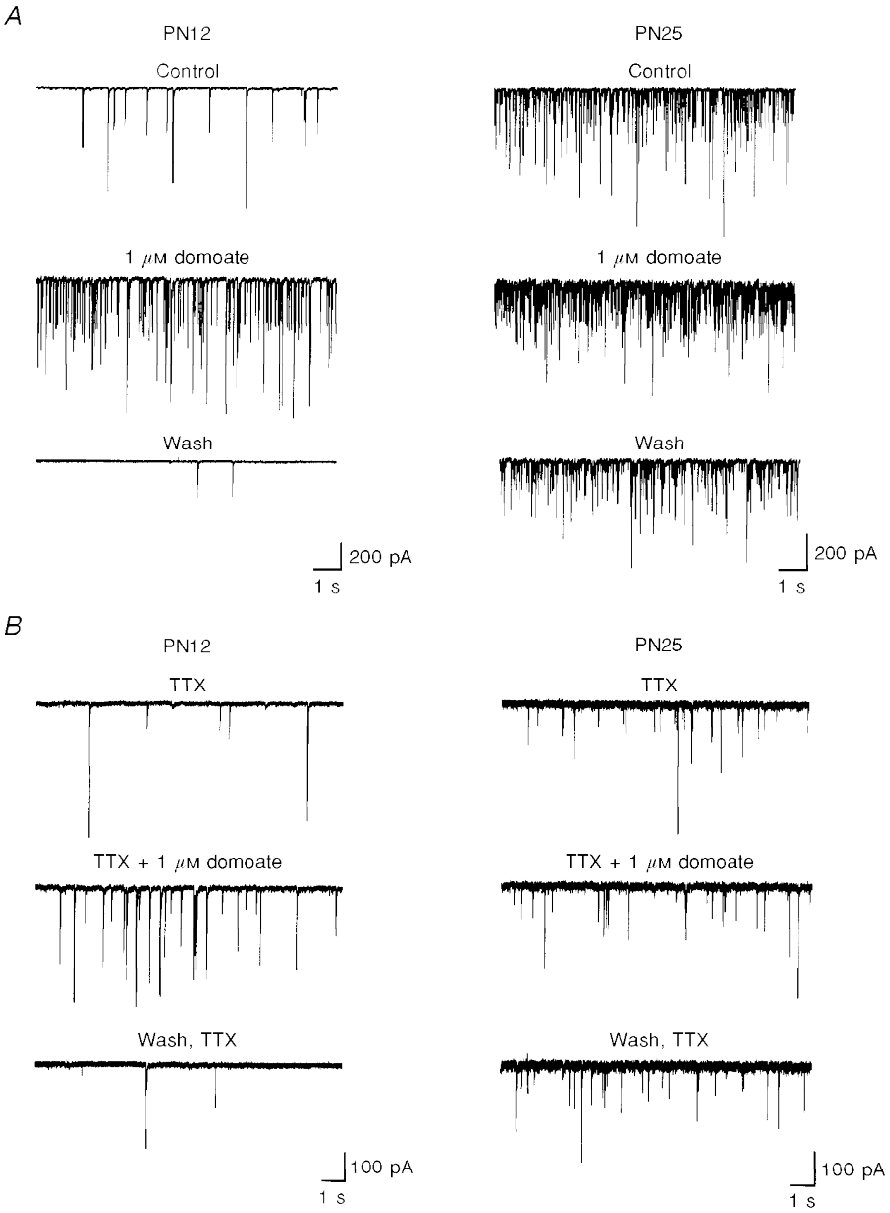

Figure 4. Changes in spontaneous and mIPSC frequency and in the effect of domoate with age
Left panels: samples of a continuous recording of IPSCs in a stellate cell in the cerebellum from a PN12 mouse. Right panels: samples of a continuous recording of IPSCs in a stellate cell in the cerebellum from a PN25 mouse. In *A*, the slices were bathed in physiological saline. In *B*, the slices were bathed in physiological saline supplemented with 500 nM TTX.

number of GABAergic connections that impinge upon a stellate cell is increased. A requirement of this hypothesis is that the probability of release at individual stellate terminals should not increase during this phase of development. In fact, a dramatic decrease in the probability of release has been reported at the interneurone–Purkinje cell synapse (Pouzat & Hestrin, 1997). If the same occurs at interneurone–interneurone synapses, the ratio of spontaneous IPSC frequency (or mIPSC) between PN21–25 and PN11–13 gives a rough estimate of the minimal factor (approximately 6) by which the number of GABAergic connections is increased.

Under control conditions, domoate (1 μM) increased spontaneous IPSC frequency by a factor which decreased from $16{\cdot}0 \pm 6{\cdot}7$ at PN11–13 ($n = 6$) to $3{\cdot}3 \pm 0{\cdot}6$ at PN21–25 ($n = 7$; $P = 0{\cdot}01$, Mann–Whitney test; Figs 4 and 5). Minimal activation of AMPARs by domoate was thus far less effective in triggering action potentials in stellate/basket cells from older mice. The developmental changes were even more striking in the presence of TTX as illustrated in Fig. 4. Potentiation of GABAergic synaptic activity in stellate cells was observed at PN12 but no potentiation was observed in stellate cells from PN25 mice. Data from a number of stellate cells at various ages are summarized in Fig. 5. In stellate cells, potentiation by domoate (1 μM) of mIPSC frequency was decreased from a factor of $8{\cdot}9 \pm 2{\cdot}4$ ($n = 13$) at PN11–13 to a factor of $1{\cdot}0 \pm 0{\cdot}1$ ($n = 7$) at PN21–25 (this value was not statistically different from 1, $P > 0{\cdot}9$; the difference between both groups was statistically significant, $P < 0{\cdot}01$; Mann–Whitney test). These experiments show a clearcut developmental change in the extent of TTX-resistant potentiation of synaptic activity by domoate.

No systematic change in the amplitude of mIPSCs was observed upon application of domoate in cells where domoate increased mIPSC frequency. The ratio of the mean amplitude of mIPSCs in the presence of domoate *versus* control saline (with TTX) was on average $1{\cdot}1 \pm 0{\cdot}1$ (range, 0·62 to 1·80; $n = 13$). GYKI 53655 (50 μM) completely antagonized the TTX-resistant effect of domoate (Fig. 6*A*). In addition, these effects of domoate in the presence of TTX were mimicked by low concentrations of AMPA (330 nM) and KA (2 μM), which increased the mIPSC frequency by a factor of $3{\cdot}7 \pm 1{\cdot}2$ ($n = 4$) and $4{\cdot}9 \pm 2{\cdot}2$ ($n = 5$), respectively (Fig. 6*B*). This suggests a presynaptic modulation of synaptic transmission by activation of AMPARs in the absence of action potential firing.

Ca^{2+} permeability of AMPARs in stellate cells and TTX-resistant potentiation of mIPSC frequency by domoate

We determined whether AMPARs located in stellate cells were permeable to Ca^{2+}, a property that could influence their ability to modulate synaptic transmission at a presynaptic level. We compared the reversal potentials of domoate-activated currents in a Na^+-rich solution and in a Ca^{2+}-rich solution (100 mM Ca^{2+}, no Na^+ in the extracellular

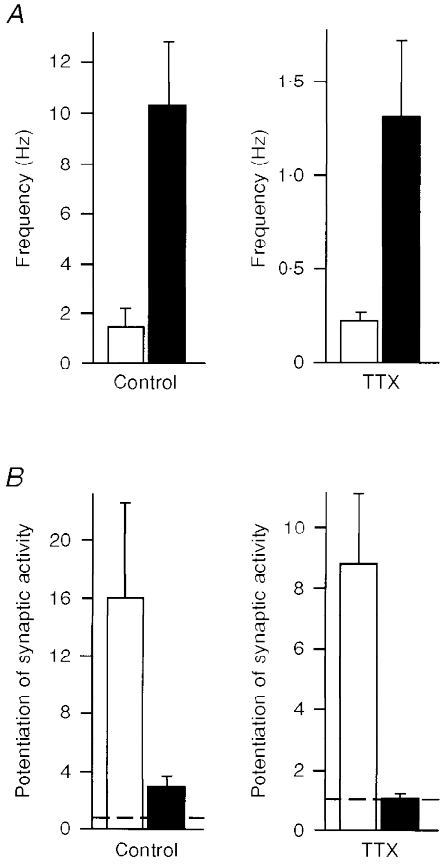

Figure 5. Summary plots of the developmental changes in GABAergic synaptic activity and in the effects of domoate
A, pooled data (means ± S.E.M.) of the mean frequency of IPSCs under control conditions (left) and in the presence of 400–500 nM TTX (right). *B*, pooled data of the potentiation of synaptic activity induced by 1 μM domoate in stellate cells under control conditions (left) and in the presence of 400–500 nM TTX (right). Mean values ± S.E.M. of the ratio of mean frequency in the test condition to that in the control are shown. In *A* and *B*: □, PN11–13 mice ($n = 6$ for control conditions, $n = 13$ for experiments with TTX); ■, PN21–25 mice ($n = 7$).

medium). These measurements could not be performed in the whole-cell mode because complete replacement of Na^+ by Ca^{2+} impaired recording. These experiments were thus performed in nucleated patches from stellate cell somata. The membrane potential was varied by 10 mV steps (100 ms; Fig. 7). When external monovalent ions were entirely replaced with 100 mM Ca^{2+}, the reversal potential shifted from $-3{\cdot}1 \pm 0{\cdot}4$ to $+1{\cdot}4 \pm 1{\cdot}2$ mV ($n = 10$; not corrected for liquid junction potentials) at PN11–13, and from $-6{\cdot}6 \pm 3{\cdot}4$ to $-6{\cdot}9 \pm 3{\cdot}9$ ($n = 7$) at PN21–25. The P_{Ca}/P_{Na} values calculated from the shift in reversal potential after correction for the liquid junction potentials were $0{\cdot}62 \pm 0{\cdot}04$ ($n = 10$) at PN11–13 and $0{\cdot}46 \pm 0{\cdot}07$ ($n = 7$) at PN21–25. These values indicate that, for both age groups, AMPARs located on stellate cells show a Ca^{2+} permeability that is severalfold higher than that of AMPARs of the type described on principal neurones in the hippocampus (Geiger *et al.* 1995).

In order to test whether the influx of Ca^{2+} through Ca^{2+}-permeable AMPARs was involved in the domoate-induced release of GABA in the presence of TTX, in PN11–13 mice, we used Cd^{2+} as a broad-spectrum voltage-gated Ca^{2+} channel antagonist. When $CdCl_2$ (100 μM) was added to the TTX-containing solution, no change in the frequency of mIPSCs was observed, suggesting that mIPSCs are not dependent on the generation of Ca^{2+}-dependent action

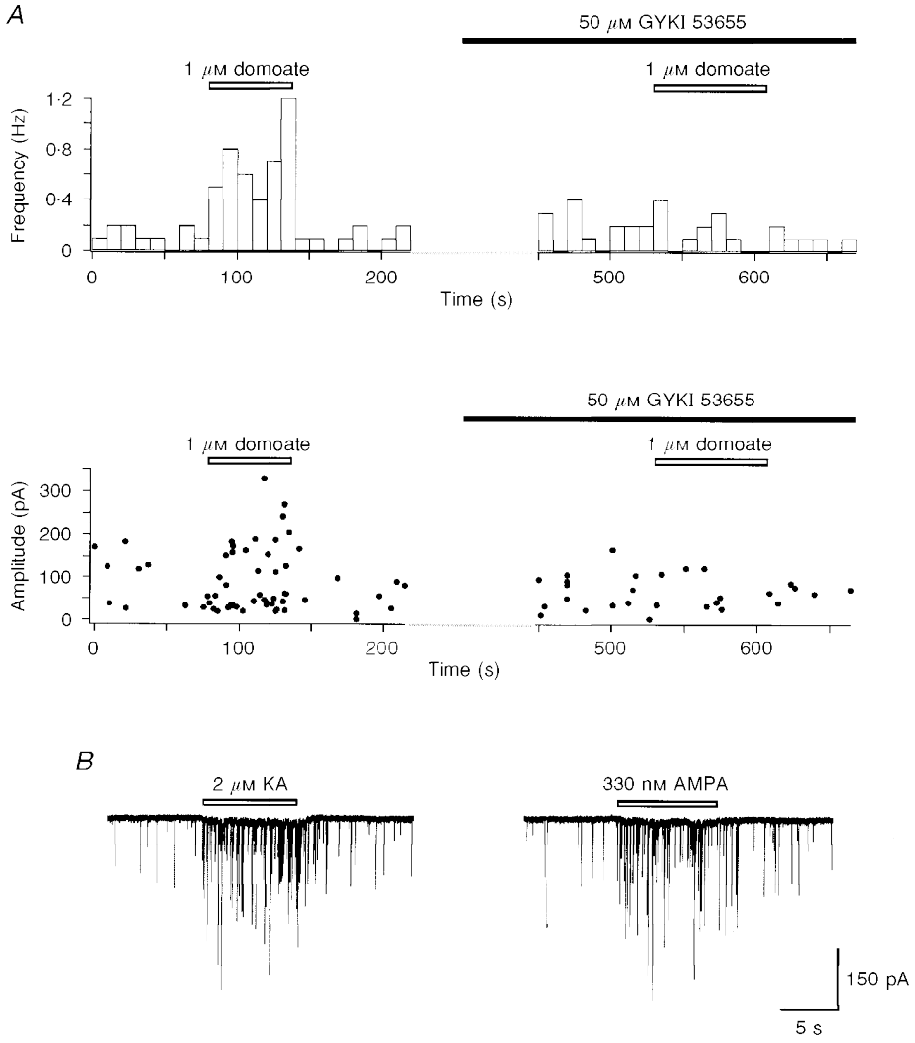

Figure 6. TTX-resistant effect of domoate on synaptic activity is blocked by GYKI 53655 and is mimicked by effects of KA and AMPA

A, upper panel: plots of the mean frequency of synaptic events detected during 10 s intervals against time. The potentiation of frequency of mIPSCs induced by 1 μM domoate was inhibited by 50 μM GYKI 53655. Lower panel: for the same cell, plots of the amplitude of each synaptic event recorded continuously. Open and filled horizontal bars indicate the time during which 1 μM domoate and 50 μM GYKI 53655 were applied, respectively. *B*, samples of a continuous recording of mIPSCs in a stellate cell. KA (2 μM) and AMPA (330 nM), applied during the time indicated by the horizontal bars, led to a reversible increase in synaptic activity in the same cell. The slice was bathed in physiological saline supplemented with 500 nM TTX. Cells from PN13 and PN12 mice were used in *A* and *B*, respectively.

potentials (Llano & Gerschenfeld, 1993*a*). However, we found a consistent decrease in the mean amplitude of mIPSCs, an effect that could be explained by a postsynaptic effect of $CdCl_2$ on $GABA_A$ receptor function, as reported for rat cerebellar interneurones (Llano & Gerschenfeld, 1993*a*). At a concentration of domoate of 1 μM, a small postsynaptic current was commonly observed that allowed us to check that $CdCl_2$, by itself, did not have any effect on postsynaptic AMPAR-mediated currents. In the presence of TTX and $CdCl_2$, the effect of domoate (1 μM) on mIPSC frequency was significantly decreased in all neurones tested by an average of $59{\cdot}5 \pm 9{\cdot}0\,\%$ ($n = 10$). Synaptic activity was potentiated by domoate by a factor of $9{\cdot}8 \pm 3{\cdot}0$ in TTX, and in the same neurones, by a factor of $2{\cdot}6 \pm 0{\cdot}5$ in TTX + $CdCl_2$ (Fig. 8; $n = 10$, Wilcoxon paired test, values significantly different, $P < 0{\cdot}01$). The residual potentiation by domoate in the presence of TTX + $CdCl_2$ was significant ($P < 0{\cdot}01$). We checked that $CdCl_2$, at a concentration of 50 μM, completely blocked evoked GABAergic synaptic transmission using a focal stimulating electrode (data not shown). These data suggest that indirect activation of voltage-gated Ca^{2+} channels is involved in the TTX-resistant effect of domoate. However, the remaining effect of domoate, observed when voltage-gated Ca^{2+} channels were blocked by $CdCl_2$, could be due to a direct influx of Ca^{2+} through Ca^{2+}-permeable AMPARs.

Focal application of domoate

In order to gain additional information as to the localization of AMPARs mediating the presynaptic action of domoate, domoate was applied focally (1 μM for 20–40 s duration) to the surface of the slice. The experiments were performed with slices from PN11–13 mice in the presence of TTX (500 nM). The puffer pipette was positioned at various sites around the recorded stellate cell body, at distances ranging from 15 to 350 μm, and the factor by which domoate increased mIPSC frequency was measured at each puffer pipette site ($n = 7$–41 puff applications per neurone). In the example shown in Fig. 9, focal application of domoate increased mIPSC frequency when the puffer pipette was positioned within a distance of 120 μm. No increase in mIPSC frequency was observed outside these limits. On average, the presynaptic action of domoate was observed within a distance of 121 ± 13 μm ($n = 15$ neurones; a TTX-resistant effect of domoate was observed in 15 out of 29 neurones tested) from the cell body. The histogram shows that the level of potentiation was stable within a radius of 120 μm from the cell body (Fig. 9*C*). At the majority ($73 \pm 10\,\%$) of puff application sites where a presynaptic effect of domoate was observed, a direct postsynaptic effect on the recorded cell was also detected. On average, the distance from the cell body up to which a postsynaptic action of domoate could be observed was 107 ± 9 μm

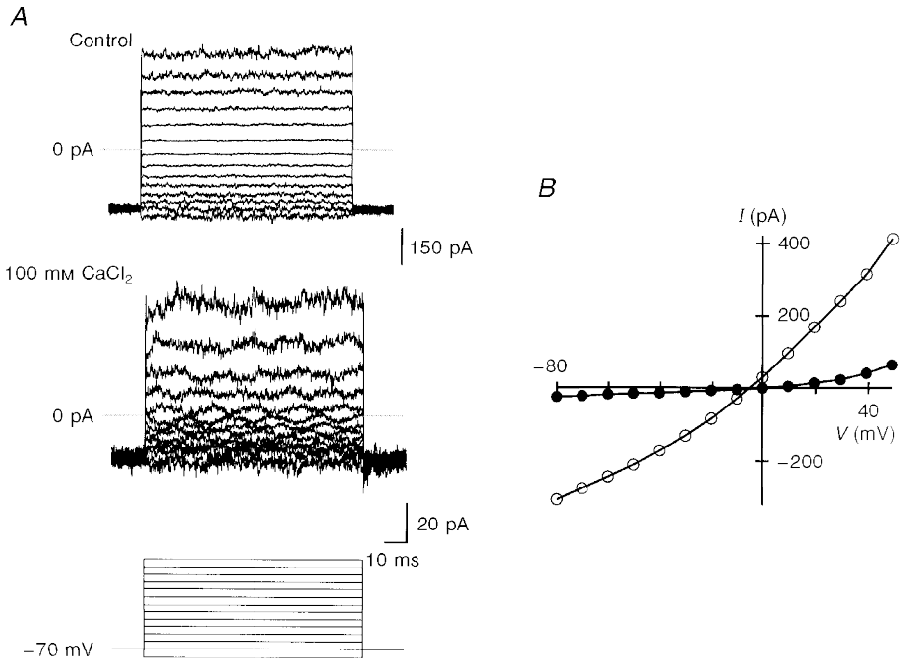

Figure 7. Ca^{2+} permeability of AMPAR channels in stellate cells

A, domoate-activated currents recorded in a nucleated patch from a stellate cell, in control (high Na^+; top traces) and in 100 mM $CaCl_2$ (middle traces). For each voltage step, current traces were generated by subtracting the traces obtained under control conditions from those obtained during application of 50 μM domoate. The voltage protocol (10 mV steps) is shown at the bottom. *B*, *I*–*V* relations of currents activated by 50 μM domoate. These data are the graphic representation of currents shown in *A*. ○, control conditions (high Na^+); ●, in 100 mM $CaCl_2$ (Na^+-free extracellular solution). These experiments were performed using cells from a PN13 mouse.

($n = 15$). These results show that the presynaptic action of domoate on GABAergic afferent neurones can be exerted without attenuation at a distance greater than 100 μm from the cell body and that the presynaptic action of domoate is observed within the area of the dendritic arborization of the recorded neurone.

We also compared the effects of focal application of domoate in the presence and absence of TTX in a set of neurones from PN11–13 mice. For all neurones tested in the absence of TTX, domoate caused a rapid increase in IPSC frequency at distances from the cell body which were on average comparable to those observed in the presence of TTX (108 ± 18 μm, $n = 10$ cells). These neurones were then tested in the presence of TTX to determine whether focally applied domoate had an effect at the sites already tested under control conditions. In only four out of these ten neurones was domoate effective in increasing mIPSC frequency. This result suggests that the presence of afferent neurones in the vicinity of the recorded stellate cell is not by itself sufficient to account for the TTX-resistant presynaptic modulation by domoate. Finally, no striking difference was observed in the effects of focally applied domoate in the absence of TTX in cells from PN11–13 and PN21–25 mice. In cells from PN21–25 mice, focal application of domoate increased the frequency of IPSCs within a mean distance of 116 ± 9 μm ($n = 3$), from the recorded cell body, implying that the spacing between connected stellate cell somata is not significantly different in slices from immature and mature mice.

DISCUSSION

In this study we show that minimal activation of AMPARs by low concentrations of domoate potentiates GABAergic synaptic activity in stellate cells in the presence of TTX. This effect of domoate was observed at immature stages in the development of stellate cells (PN11–13), but not at more mature stages (after PN21). We discuss the possibility that this presynaptic modulation of GABAergic transmission can be due either to an axonal/presynaptic localization of AMPARs or to specific properties of immature stellate cell axons.

Potentiation of GABAergic synaptic transmission by minimal activation of AMPARs

Domoate and KA are agonists at both AMPARs and KARs. Domoate and KA, at submicromolar concentrations, are potent neurotoxic agents whose toxicity is thought to be mediated by an ionotropic receptor with a high affinity for KA. However, because of the lack of specific agonists and antagonists for KARs, it is still not clear whether the neurotoxic effects of KA and domoate are due to the activation of AMPARs or of KARs. Both agonists display a higher affinity for KARs than for AMPARs. Using domoate as an agonist, expression studies of recombinant AMPARs and KARs have obtained EC_{50} values of lower than 1 μM for GluR5 and GluR6, and of the order of 50 μM for GluR3 (Sommer, Burnashev, Verdoorn, Keinänen, Sakmann & Seeburg, 1992; Stern-Bach, Bettler, Hartley, Sheppard, O'Hara & Heinemann, 1994; Bettler & Mulle, 1995). Studies of the efficacy of domoate on native AMPARs and KARs

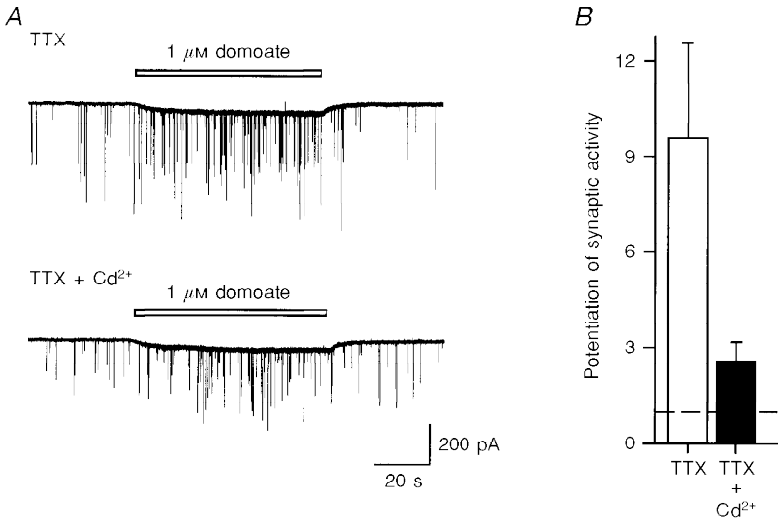

Figure 8. $CdCl_2$ partially blocks the potentiation of mIPSC frequency induced by domoate in stellate cells

A, samples of a continuous recording of mIPSCs in a stellate cell. $CdCl_2$ (100 μM) decreased the effect of 1 μM domoate, applied during the time indicated by the horizontal bars, on mIPSC frequency without affecting the direct postsynaptic current. *B*, pooled data of the potentiation of synaptic activity induced by 1 μM domoate in stellate cells. □, data from experiments carried out in the presence of 500 nM TTX; ■, data from experiments carried out in the presence of 500 nM TTX and 100 μM $CdCl_2$ ($n = 10$). Mean values ± S.E.M. of the ratio of mean frequency in the test condition to that in the control are shown. All experiments were performed using cells from PN11–13 mice.

have yielded comparative results (Huettner, 1990; Patneau & Mayer, 1990). Domoate activates a slowly desensitizing AMPAR current and a more rapidly desensitizing KAR current. Recent work has led to the conclusion that low concentrations of KA activate KARs and not AMPARs in CA3 hippocampal neurones (Castillo *et al.* 1997). Although domoate potentiates GABAergic synaptic activity in cerebellar stellate cells at submicromolar concentrations, these effects are probably not mediated by KARs but more likely by AMPARs, for several reasons. First, both the TTX-dependent and the TTX-resistant effects of domoate on IPSC frequency were completely blocked by 50 μM GYKI 53655, which also fully blocks EPSCs evoked in stellate cells by parallel fibre stimulation (data not shown). As a selective antagonist of AMPARs, GYKI 53655 (LY300518) has proved useful in distinguishing AMPAR- from KAR-mediated physiological responses (Paternain *et al.* 1995; Castillo *et al.* 1997; Vignes & Collingridge, 1997). In addition, both the TTX-dependent and TTX-resistant effects of domoate were mimicked by AMPA. Moreover, the effects of domoate and KA on IPSC frequency, as well as on the postsynaptic currents activated by higher concentrations of the agonists, did not show desensitization under our conditions. These findings would be inconsistant with an activation of KARs (see Bettler & Mulle (1995) for review). Finally, stellate cells show a high level of expression of the GluR7 KAR subunit gene; while this study was in progress, recombinant GluR7 receptors were shown to form functional channels that were not sensitive to domoate (Schiffer, Swanson & Heinemann, 1997).

Mechanisms for the presynaptic modulation of GABAergic synaptic transmission by domoate

We have shown that domoate increases GABAergic synaptic activity while only activating small AMPAR-mediated postynaptic currents. Domoate (100–500 nM) triggered action potential firing in presynaptic stellate cells, while in all stellate cells tested in the whole-cell mode, it activated a postsynaptic current of a few picoamps. Stellate cells are electrically compact neurones displaying an average input

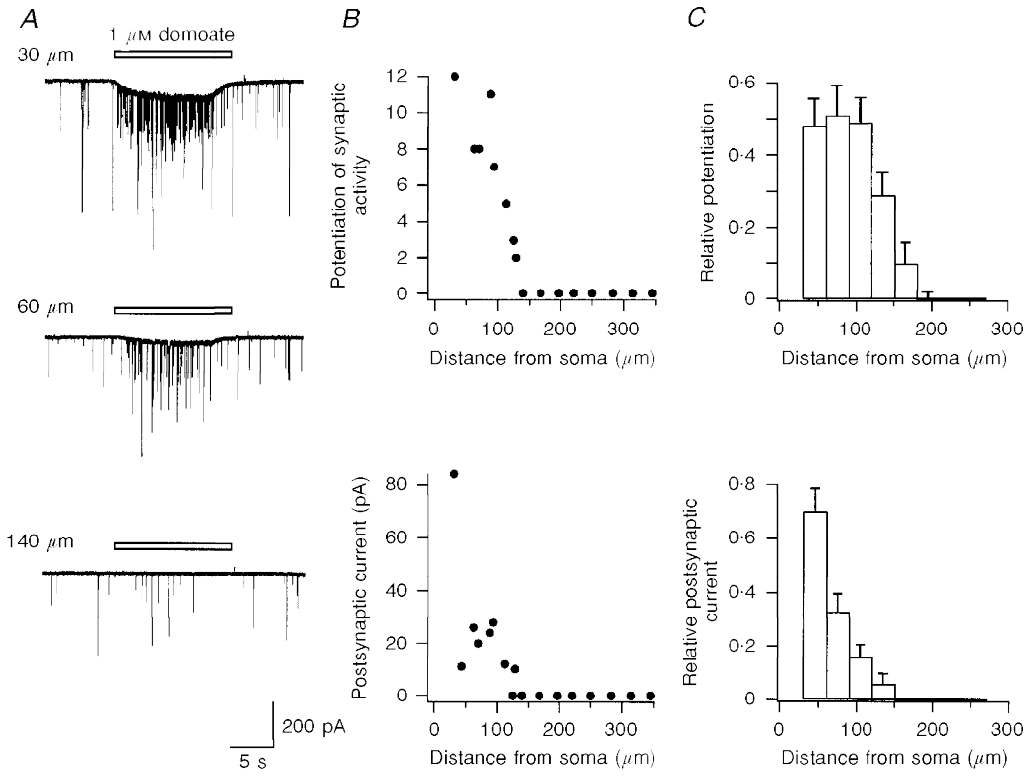

Figure 9. Focal application of domoate increases the frequency of mIPSCs in stellate cells

A, samples of a continuous recording of mIPSCs in a stellate cell in the cerebellum from a PN13 mouse. In the presence of TTX (500 nM), focal application of 1 μM domoate, indicated by the horizontal bars above the traces, increased mIPSC frequency when applied at a distance of 30 μm from the soma of the recorded stellate cell. This effect was decreased at 60 μm and was not observed at 140 μm. *B* shows, in the same cell, plots of the effects of focal application of domoate on mIPSC frequency, as measured by the ratio of mIPSC frequency in the test condition to that in the control (top), and postsynaptic current (bottom), as a function of the distance from the recorded stellate cell. *C*, pooled data for the effects of focal application of domoate (1 μM) on mIPSC frequency (top) and postsynaptic current (bottom). On the ordinate, values are given relative to the maximal potentiation and maximal postsynaptic current measured for each cell. All experiments were performed using cells from PN11–13 mice ($n = 15$).

resistance of 863 MΩ when measured in the current-clamp mode. Thus, a 5 pA inward current will cause on average a 4·3 mV depolarization of the membrane. A small domoate-activated postsynaptic current is thus sufficient to depolarize presynaptic interneurones to action potential threshold.

More interestingly, in immature stellate cells, domoate increased IPSC frequency even in the presence of TTX, which blocks action potentials in all presynaptic neurones. An increase in mIPSC frequency by an ionotropic receptor agonist is generally thought to be mediated by the activation of presynaptic receptors (see, e.g. Gray, Rajan, Radcliffe, Yakehiro & Dani, 1996; Léna & Changeux, 1997; Gu & MacDermott, 1997). Thus, an explanation for the TTX-resistant effect of domoate is that, in immature neurones, AMPARs mediating the effect of domoate are located close to synaptic releases sites. In several instances, ionotropic receptors involved in the modulation of transmitter release, i.e. nicotinic receptors (Gray *et al.* 1996; Léna & Changeux, 1997), are known to be permeable to Ca^{2+}. It has been proposed that Ca^{2+} entering through the receptor channel could directly influence synaptic release. The value of P_{Ca}/P_{Na} for AMPARs on stellate cells (0·62 at PN11–13 and 0·46 at PN21–25) is severalfold higher than that of AMPARs found on principal neurones (CA3 pyramidal cells: $P_{Ca}/P_{Na} = 0{\cdot}1$; or dentate gyrus granule cells: $P_{Ca}/P_{Na} = 0{\cdot}09$), and is comparable with the values reported for non-pyramidal neocortical neurones ($P_{Ca}/P_{Na} = 0{\cdot}69$; Geiger *et al.* 1995) and globus pallidus neurones ($P_{Ca}/P_{Na} = 0{\cdot}67$; Götz, Kraushaar, Geiger, Lubke, Berger & Jonas, 1997). It is, however, lower than the values reported for hippocampal type II cultured neurones ($P_{Ca}/P_{Cs} = 2{\cdot}3$; Iino, Ozawa & Tsuzuki, 1990) or hippocampal basket cells ($P_{Ca}/P_{Na} = 1{\cdot}79$; Koh, Geiger, Jonas & Sakmann, 1995). The finding that AMPARs on stellate cells are Ca^{2+} permeable is in agreement with recent immunocytochemical studies showing a lack of labelling of these neurones with a GluR2 subunit-selective antibody (Petralia *et al.* 1997). The question arises as to whether Ca^{2+} directly entering through the AMPAR channels plays a role in modulating synaptic transmission. In the presence of TTX, Cd^{2+} attenuated the effect of domoate on mIPSC frequency without affecting the amplitude of AMPAR-mediated postsynaptic currents, implying that voltage-dependent Ca^{2+} channels are involved in the TTX-resistant effect of domoate. Depolarization of the membrane in the axon terminal following the opening of AMPARs probably activates presynaptic voltage-dependent Ca^{2+} channels, leading to enhanced transmistter release. However, under experimental conditions in which Ca^{2+} entry through voltage-gated channels was blocked by Cd^{2+}, domoate significantly increased mIPSC frequency. This result suggests that Ca^{2+} directly entering through the AMPAR channels could also participate in the TTX-resistant modulation of synaptic transmission by domoate. In addition, this role of Ca^{2+} lends support to the notion that AMPARs mediating presynaptic modulation should be located close to GABA release sites.

In order to gain more information on the localization of AMPARs that mediate the increase in mIPSC frequency, domoate was focally applied to the surface of the slice of the immature cerebellum. We show that the effect of focally applied domoate was not restricted to the soma and proximal dendrites, as would be expected if presynaptic AMPARs were located on axon terminals with GABAergic synapses distributed close to the cell body. Indeed, focally applied domoate increased mIPSC frequency at distances up to 120 μm from the recorded cell body. In the same experiments, focally applied domoate activated AMPAR-mediated postsynaptic currents at distances up to 100 μm from the recorded cell body. There is a high topographical correlation between the sites at which domoate activated AMPAR-mediated postsynaptic currents and the sites at which it increased mIPSC frequency, suggesting a topographical correlation between the presence of post-synaptic dendrites and AMPARs involved in the presynaptic modulation of transmitter release. This result opens the possibility of AMPARs being located close to synaptic release sites with GABAergic synapses being distributed on proximal as well as distal dendrites. It has been shown that stellate cells make GABAergic synapses at the level of dendrites (Nusser, Cull-Candy & Farrant, 1997), although no data are available as to the distance from the cell body at which synapses are made.

Although glutamate receptor-mediated excitation has been reported in intracellular and patch-clamp recordings of lamprey reticulospinal axons, demonstrating the presence of glutamate receptors in axons (Cochilla & Alford, 1997), a definitive answer for the presence of AMPARs on axons and presynaptic terminals in rodents would require a morphological demonstration. Immunocytochemical localization studies indicate a predominant somato-dendritic localization of AMPARs in adult rat brain (Petralia & Wenthold, 1992; Martin, Blackstone, Levey, Huganir & Price, 1993) as well as in mature hippocampal neurones in culture (Craig, Blackstone, Huganir & Banker, 1993; Eshhar, Petralia, Winters, Niedzielski & Wenthold, 1993). Only occasional staining of axons is encountered in the adult rat brain, with no evidence for labelling of presynaptic terminals. However, at early stages of maturation in culture, GluR1 and GluR2/3 are reported to be relatively uniformly distributed in cell bodies, axons and minor processes (Craig *et al.* 1993). They become restricted to somato-dendritic domains at later stages of neuronal maturation in culture (Jones & Baughman, 1991; Craig *et al.* 1993; Eshhar *et al.* 1993). Our data bring a physiological counterpart to these observations made in hippocampal cultures and they suggest that, at early stages of maturation, AMPARs could be located in the axonal as well as the somato-dendritic compartment.

An alternative explanation for the TTX-resistant effects of domoate on synaptic transmission is that the minimal activation of AMPARs located in somato-dendritic compartments could be effective in depolarizing the axon

terminals either directly or by generating Ca^{2+}-dependent action potentials. There is no evidence for the existence of Ca^{2+}-dependent action potentials in stellate neurones (Llano & Gerschenfeld, 1993*a*; this study), and Cd^{2+} does not block completely the TTX-resistant effect of domoate. We have found that focally applied domoate is effective, on average, within similar distances in the presence and in the absence of TTX. These experiments also suggest that presynaptic stellate cells are located in the same area (as judged by increase in IPSC frequency in the absence of TTX) as the dendritic arborization (as judged by the presence of AMPAR-mediated postsynaptic currents). A requirement of the hypothesis of a direct depolarization would be that a small (< 5 mV) somato-dendritic depolarization could be electrotonically propagated to axon terminals to trigger voltage-dependent Ca^{2+} entry. If such was the case, we would expect to observe a TTX-resistant effect of domoate in more mature stellate cells, for the following reasons. The distance between connected stellate cells (thus axonal length) does not change dramatically between PN11–13 and PN21–25. Indeed, experiments using focal application of domoate showed that presynaptic neurones are located within similar distances from the recorded stellate cell in cerebellum slices from immature and mature mice. In addition, axonal length does not seem to change dramatically between PN15 and the adult stage in the rat (C. Pouzat & S. Kondo, personal communication). Finally, AMPARs are present on immature as well as mature stellate cell somata, as judged from the amplitude of currents activated by domoate in nucleated patches excised from the soma. In immature stellate cells, by comparing the effects of focal application of domoate on cells in the absence and presence of TTX, we have shown that the presence of connected presynaptic neurones close to the recorded cell does not imply a TTX-resistant increase in IPSC frequency in all cases.

Synaptic transmission between stellate/basket cells is also potentiated by the activation of metabotropic glutamate receptors (Llano & Marty, 1995). t-ACPD ((±)-1-aminocyclopentane-*trans*-1,3-dicarboxylic acid), a general glutamate metabotropic agonist, enhances the frequency of spontaneous IPSCs as well as the frequency of action potentials in interneurones of the molecular layer, in 10- to 16-day-old rats. However, unlike domoate, t-ACPD does not affect the frequency of mIPSCs, suggesting that it only acts by increasing the excitability of the presynaptic interneurones and does not act at the level of axon terminals. The frequency of mIPSCs in rat stellate cells was also shown to be enhanced by noradrenaline (Llano & Gerschenfeld, 1993*b*), but the mechanism of modulation of transmitter release involved is different from that of domoate, since it is not attenuated by Cd^{2+} and probably involves protein kinase A (Kondo & Marty, 1997).

Developmental changes in the effects of domoate

An important aspect of these results is that the presynaptic modulation of GABAergic synaptic transmission is subject to a clear developmental switch. We observed that the effects of domoate on spontaneous and mIPSCs were prevalent at PN11–13 and declined dramatically over the next 2 weeks of development. Domoate did not increase mIPSC frequency at PN21–25. A shift in the subcellular localization of AMPARs during this period of maturation appears to be a relevant interpretation of the disappearance of the TTX-resistant effect of domoate. Alternative explanations for the developmental changes in the TTX-resistant effects of domoate include a change in the properties of stellate cell axons, a change in the properties of the interneurone–interneurone synapse or a change in the properties of AMPARs. No data are available regarding a developmental change in the properties of stellate cell axons. Nevertheless, our experiments using focal application of domoate showed that the distance beween connected stellate cells – related to axonal length – does not change dramatically between PN11–13 and PN21–25. A phenomenon of saturation of the probability of release could alternatively occur at synapses between mature stellate cells. This latter possibility seems unlikely since, on the contrary, a decrease in the probability of release at individual interneurone terminals during the course of maturation has been reported (Pouzat & Hestrin, 1997). Finally, AMPARs in stellate cells are permeable to Ca^{2+} in both PN11–13 and PN21–25 mice, although a slight decrease in P_{Ca}/P_{Na} is observed in the older group.

In summary, our data raise the possibility that AMPARs are located close to synaptic terminals in immature stellate cells. During maturation, AMPARs would become restricted to soma and dendrites, accounting for the lack of effect of AMPAR activation on the potentiation of mIPSC frequency. Overall, minimal activation of AMPARs increases inhibitory synaptic activity of immature cerebellar interneurones. These findings correlate with the role of endogenous glutamate during a comparable period of cerebellar development via activation of NMDA receptors (Komuro & Rakic, 1993; Rossi & Slater, 1993). The concentration of glutamate in the extracellular space fluctuates during physiological processes in the micromolar range. Given the very low concentrations of domoate found to be effective in modulating transmitter release in stellate cells, it is tempting to speculate that, in the immature cerebellum, extrasynaptic AMPARs are also activated by ambient glutamate and as a consequence modulate the activity of the interneuronal network.

Altman, J. & Bayer, S. A. (1997). *Development of the Cerebellar System in Relation to its Evolution, Structure and Functions*. CRC Press, Boca Raton, FL, USA.

Ankri, N., Legendre, P., Faber, D. S. & Korn, H. (1994). Automatic detection of spontaneous synaptic responses in central neurones. *Journal of Neuroscience Methods* **52**, 87–100.

Baude, A., Molnar, E., Latawiec, D., McIlhinney, R. A. & Somogyi, P. (1994). Synaptic and nonsynaptic localization of the GluR1 subunit of the AMPA-type excitatory amino acid receptor in the rat cerebellum. *Journal of Neuroscience* **14**, 2830–2843.

Bettler, B., Egebjerg, J., Sharma, G., Pecht, G., Hermans-Borgmeyer, I., Moll, C., Stevens, C. F. & Heinemann, S. (1992). Cloning of a putative glutamate receptor: a low affinity kainate receptor subunit. *Neuron* **8**, 257–265.

Bettler, B. & Mulle, C. (1995). AMPA and kainate receptors. *Neuropharmacology* **34**, 123–139.

Castillo, P. E., Malenka, R. C. & Nicoll, R. A. (1997). Kainate receptors mediate a slow postsynaptic current in hippocampal CA3 neurons. *Nature* **388**, 182–186.

Chittajallu, R., Vignes, M., Dev, K. K., Barnes, J. M., Collingridge, G. L. & Henley, J. M. (1996). Regulation of glutamate release by presynaptic kainate receptors in the hippocampus. *Nature* **379**, 78–81.

Cochilla, A. J. & Alford, S. (1997). Glutamate receptor-mediated synaptic excitation in axons of the lamprey. *Journal of Physiology* **499**, 443–457.

Craig, A. M., Blackstone, C. D., Huganir, R. L. & Banker, G. (1993). The distribution of glutamate receptors in cultured rat hippocampal neurons: postsynaptic clustering of AMPA selective subunits. *Neuron* **10**, 1055–1068.

Edwards, F. A., Konnerth, A., Sakmann, B. & Takahashi, T. (1989). A thin slice preparation for patch-clamp recordings from neurones of the mammalian central nervous system. *Pflügers Archiv* **414**, 600–612.

Eshhar, N., Petralia, R. S., Winters, C. A., Niedzielski, A. S. & Wenthold, R. J. (1993). The segregation and expression of glutamate receptor subunits in cultured hippocampal neurons. *Neuroscience* **57**, 943–964.

Gaiarsa, J.-L., Zagrean, L. & Ben-Ari, Y. (1994). Neonatal irradiation prevents the formation of hippocampal mossy fibers and the epileptic action of kainate on rat CA3 pyramidal neurons. *Journal of Neurophysiology* **71**, 204–215.

Geiger, J., Melcher, T., Koh, D.-S., Sakmann, B., Seeburg, P., Jonas, P. & Monyer, H. (1995). Relative abundance of subunit mRNAs determines gating and Ca^{2+} permeability of AMPA receptors in principal neurons and interneurons in rat CNS. *Neuron* **15**, 193–204.

Götz, T., Kraushaar, U., Geiger, J., Lubke, J., Berger, T. & Jonas, P. (1997). Functional properties of AMPA and NMDA receptors expressed in identified types of basal ganglia neurons. *Journal of Neuroscience* **17**, 204–215.

Gray, R., Rajan, A., Radcliffe, K., Yakehiro, M. & Dani, J. A. (1996). Hippocampal synaptic transmission enhanced by low concentrations of nicotine. *Nature* **383**, 713–716.

Gu, J. G. & MacDermott, A. B. (1997). Activation of ATP P2X receptors elicits glutamate release from sensory neuron synapses. *Nature* **389**, 749–753.

Huettner, J. E. (1990). Glutamate receptor channels in rat DRG neurons: activation by kainate and quisqualate and blockade of desensitization by Con A. *Neuron* **5**, 255–266.

Iino, M., Ozawa, S. & Tsuzuki, K. (1990). Permeation of calcium through excitatory amino acid receptor channels in cultured rat hippocampal neurones. *Journal of Physiology* **424**, 151–165.

Jones, K. A. & Baughman, R. W. (1991). Both NMDA and non-NMDA subtypes of glutamate receptors are concentrated at synapses on cerebral cortical neurons in culture. *Neuron* **7**, 593–603.

Keinänen, K., Wisden, W., Sommer, B., Werner, P., Herb, H., Verdoorn, T. A., Sakmann, B. & Seeburg, P. H. (1990). A family of AMPA-selective glutamate receptors. *Science* **249**, 556–560.

Koh, D.-S., Geiger, J. R. P., Jonas, P. & Sakmann, B. (1995). Ca^{2+}-permeable AMPA and NMDA receptor channels in basket cells of rat hippocampal dentate gyrus. *Journal of Physiology* **485**, 383–402.

Komuro, H. & Rakic, P. (1993). Modulation of neuronal migration by NMDA receptors. *Science* **260**, 95–97.

Kondo, S. & Marty, A. (1997). Protein kinase A-mediated enhancement of miniature IPSC frequency by noradrenaline in rat cerebellar stellate cells. *Journal of Physiology* **498**, 165–176.

Léna, C. & Changeux, J.-P. (1997). Role of Ca^{2+} ions in nicotinic facilitation of GABA release in mouse thalamus. *Journal of Neuroscience* **17**, 576–585.

Llano, I. & Gerschenfeld, H. M. (1993*a*). Inhibitory synaptic currents in stellate cells of rat cerebellar slices. *Journal of Physiology* **468**, 177–200.

Llano, I. & Gerschenfeld, H. M. (1993*b*). β-Adrenergic enhancement of inhibitory synaptic activity in rat cerebellar stellate and Purkinje cells. *Journal of Physiology* **468**, 201–224.

Llano, I. & Marty, A. (1995). Presynaptic metabotropic regulation of inhibitory synapses in rat cerebellar slices. *Journal of Physiology* **486**, 163–176.

Martin, L., Blackstone, C., Levey, A., Huganir, R. & Price, D. (1993). AMPA glutamate receptor subunits are differentially distributed in rat brain. *Neuroscience* **53**, 327–358.

Nusser, Z., Cull-Candy, S. & Farrant, M. (1997). Differences in synaptic GABA(A) receptor number underlie variation in GABA mini amplitude. *Neuron* **19**, 697–709.

Palay, S. L. & Chan-Palay, V. (1974). *Cerebellar Cortex*: *Cytology and Organization*. Springer, Berlin.

Paternain, A., Morales, M. & Lerma, J. (1995). Selective antagonism of AMPA receptor unmasks kainate receptor-mediated responses in hippocampal neurons. *Neuron* **14**, 185–189.

Patneau, D. & Mayer, M. (1990). Structure–activity relationships for amino acid transmitter candidates acting at *N*-methyl-D-aspartate and quisqualate receptors. *Journal of Neuroscience* **10**, 2385–2399.

Petralia, R. S., Wang, Y., Mayat, E. & Wenthold, R. J. (1997). Glutamate receptor subunit 2-selective antibody shows a differential distribution of calcium permeable AMPA receptors among populations of neurons. *Journal of Comparative Neurology* **385**, 456–476.

Petralia, R. S. & Wenthold, R. J. (1992). Light and electron immunocytochemical localization of AMPA-selective glutamate receptors in the rat brain. *Journal of Comparative Neurology* **318**, 329–354.

Pouzat, C. & Hestrin, S. (1997). Developmental regulation of basket/stellate cell --> Purkinje cell synapses in the cerebellum. *Journal of Neuroscience* **17**, 9104–9112.

Represa, A., Tremblay, E. & Ben-Ari, Y. (1987). Kainate binding sites in the hippocampal mossy fibers: localization and plasticity. *Neuroscience* **20**, 739–748.

Rossi, D. J. & Slater, N. T. (1993). The developmental onset of NMDA-receptor channel activity during neuronal migration. *Neuropharmacology* **32**, 1239–1248.

Sather, W., Dieudonné, S., MacDonald, J. F. & Ascher, P. (1992). Activation and desensitization of *N*-methyl-D-aspartate receptors in nucleated outside-out patches from mouse neurons. *Journal of Physiology* **450**, 643–672.

Sato, K., Kiyama, H. & Tohyama, M. (1993). The differential expression patterns of messenger RNAs encoding non-NMDA glutamate receptor subunits (GluR1-4) in the rat brain. *Neuroscience* **52**, 515–539.

Schiffer, H. H., Swanson, G. T. & Heinemann, S. F. (1997). Rat GluR7 and a carboxy-terminal splice variant, GluR7b, are functional kainate receptor subunits with a low sensitivity to glutamate. *Neuron* **19**, 1141–1146.

Sommer, B., Burnashev, N., Verdoorn, T. A., Keinänen, K., Sakmann, B. & Seeburg, P. H. (1992). A glutamate receptor with high affinity for domoate and kainate. *EMBO Journal* **11**, 1651–1656.

Stern-Bach, Y., Bettler, B., Hartley, M., Sheppard, P., O'Hara, P. J. & Heinemann, S. F. (1994). Agonist selectivity of glutamate receptors is specified by two domains structurally related to bacterial amino acid-binding proteins. *Neuron* **13**, 1345–1357.

Vignes, M. & Collingridge, G. L. (1997). The synaptic activation of kainate receptors. *Nature* **388**, 179–182.

Wisden, W. & Seeburg, P. (1993). A complex mosaic of high-affinity kainate receptors in rat brain. *Journal of Neuroscience* **13**, 3582–3598.

Corresponding author

C. Mulle: CNRS UMR 5541, Université Victor Segalen-Bordeaux 2, 146 rue Léo-Saignat, 33076 Bordeaux, France.

Email: mulle@hippocrate.u-bordeaux2.fr